Kinematic geometry of spatial RSSR mechanisms

Mirja Rotzoll[a], Margaret H. Regan[b], Manfred L. Husty[c], M. John D. Hayes[a,*]

[a] *Carleton University, 1125 Colonel By Drive, Ottawa, ON K1S 5B6, Canada*
[b] *Duke University, 120 Science Drive Physics 117, Durham, NC 27708, U.S.A.*
[c] *University of Innsbruck, Technikerstraße 13, 6020 Innsbruck, Austria*

Abstract

In this paper, two different novel methods to derive the input-output (IO) equation of arbitrary RSSR linkages are described. Both methods share some common elements, i.e., they use the standard Denavit-Hartenberg notation to first describe the linkage as an open kinematic chain, and Study's kinematic mapping to describe the displacement of the coordinate frame attached to the end-effector of the chain with respect to the relatively non-moving base frame. The kinematic closure equation is obtained in the seven-dimensional projective kinematic mapping image space by equating the eight Study soma coordinates to the identity array. Then two methods are successfully applied to eliminate the intermediate joint angle parameters leading to the degree four biquadratic implicit algebraic IO equation: a) the linear implicitisation algorithm, which can be applied after rearranging the closure equation such that the linkage can be viewed as two serial RS chains, and b) numerical elimination theory using pseudowitness sets. Both approaches lead to the same IO equation. A geometric model was created in GeoGebra which verifies the derived equation.

Keywords: RSSR linkage, Study soma coordinates, algebraic input-output equation, linear implicitisation algorithm.

*Corresponding Author
Email address: `john.hayes@carleton.ca` (M. John D. Hayes)

September 2, 2022

1. Introduction

Four-bar linkages have attracted the curiosity of countless people in research and industry. The high interest in the linkage motions is not least due to the wide range of applications in which they are used today, see, for example, [1, 2]. Although there exists detailed trigonometric analysis of four-bar linkages' kinematic behaviour [3, 4], the rise of computational capacities and the rediscovery of Study's kinematic mapping [5] pose a valid reason to reinvestigate these types of linkages from an algebraic standpoint. The whole idea behind Study's kinematic mapping is to describe distinct three-dimensional displacements of a moving end-effector frame of a kinematic chain of rigid bodies as distinct points in a seven-dimensional projective kinematic mapping image space described by eight homogeneous coordinates. Constraints on the motion of the end-effector frame imposed by the joints in the kinematic chain map to curves or surfaces in the image space. The equations of these curves or surfaces are known as constraint equations [6]. The coordinate transformation of this mapping is expressed via dual quaternions instead of traditional matrix formulations. Detailed understanding of the mathematical tools that allow one to manipulate the algebraic constraint equations in Study's kinematic image space can help to solve more complex motions of kinematic chains, such as [7, 8].

One major advantage of analysing linkages using algebraic constraint equations compared to the classical trigonometric approach lies in its capability to obtain all possible solutions [9]. Motivated by these considerations, a derivation algorithm that describes the linkage using Denavit Hartenberg (DH) parameters, projects the displacement transformation matrix into Study's kinematic image space, and manipulates the resulting equations via Gröbner bases to obtain the algebraic input-output (IO) equation for planar, spherical, and Bennett linkages has been presented in [10, 11], respectively. A natural extension of this algorithm, to demonstrate its effectiveness, is to apply it to another well-investigated spatial linkage, the RSSR, which will be the main contribution of this paper. In addition, the results obtained using the polynomial elimination method [12] are supported by a numerical method [9] leading to an identical algebraic IO equation, as well as a verification of the equation using an animated example linkage that we created in the GeoGebra software.

The RSSR linkage consists of two revolute (R) and two spherical (S) joints and following the Kutzbach criterion, possesses 2 degrees of freedom (dof). However, one dof that does not influence the IO equation corresponds to the rotation of the coupler link between the two spherical joints about its own longitudinal axis. This so-called idle dof can have a positive effect on the durability of the linkage in engineering applications, as it helps to evenly wear the S joints [13]. Generally, the IO equation of the RSSR is a much more involved equation compared to the planar, and spherical ones, as in addition to the link lengths between the four joints, the linkage further possesses three additional design parameters between the revolute joints, i.e., two link offsets and a link twist. Previous trigonometric derivations of the RSSR IO equation are available, for example, in [4, 14]. Hartenberg and Denavit's derivation of the IO equation [14] uses their well-known parameters and trigonometric relations, leading to an equation that resembles a more complex version of the Freudenstein equation [3]. This is not entirely surprising given that the planar four-bar is a special case of the RSSR linkage [4, 15].

2. Denavit-Hartenberg (DH) Parametrisation

The literature contains many variations of the original Denavit-Hartenberg (DH) coordinate system and parameter assignment convention [16]. For example, subtly different coordinate frame attachment rules and parameter definitions have been devised for mechanical system calibration, dynamic analysis, accounting for misalignment of joint axis directions, etc., see [17, 18, 19, 20] for several examples. Therefore, it is important to precisely define the convention used in this work to avoid confusion and misinterpretation since the corresponding coordinate transformations are all different from those of Denavit and Hartenberg.

The first step in the DH parametrisation of an arbitrary kinematic chain is to identify and number all the joint axes. Next comes the allocation of coordinate systems to each link in the chain using a set of rules to locate the origin of the coordinate system and the orientation of the basis vectors. The position and orientation of consecutive links are defined by a homogeneous transformation matrix that maps coordinates of points in the coordinate system attached to link i to those of the same points described in the coordinate system attached to link $i-1$. Symbolically, the coordinate transformation matrix is denoted

$$ {}^{i-1}_{i}\mathbf{T}. $$

The forward and inverse kinematics of serial chains are the concatenations of the individual transformation matrices in the appropriate order [21]. For example, the forward kinematics problem of determining the position and orientation of the n^{th} link in a serial kinematic chain described in a relatively fixed non-moving base coordinate system 0, given the relevant DH parameters and values for the n joint variables is conceptually straightforward as matrix multiplication.

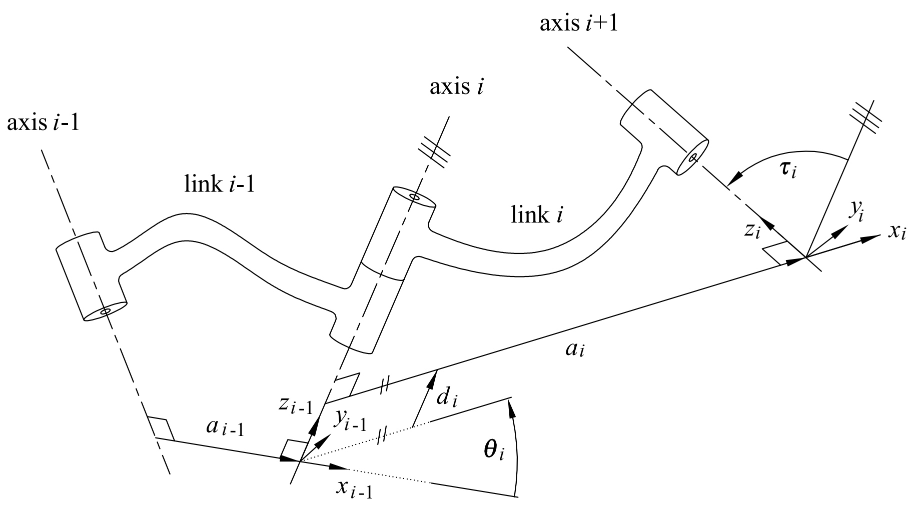

Figure 1: DH parameters in a general serial 3R kinematic chain.

To visualise the four DH parameters, consider two arbitrary sequential neighbouring links, $i-1$ and i. Two such links are illustrated, together with their

DH parameters, in Fig. 1. The DH parameters [16] are defined in the following way.

θ_i, joint angle: the angle from x_{i-1} to x_i measured about z_{i-1}.

d_i, link offset: the distance from x_{i-1} to x_i measured along z_{i-1}.

τ_i, link twist: the angle from z_{i-1} to z_i measured about x_i.

a_i, link length: the directed distance from z_{i-1} to z_i measured along x_i.

The procedure for assigning the location of the origin and the basis vector directions for the coordinate system for the i^{th} link in which the DH parameters are defined is as follows.

1. Identify all joint axes. Consider neighbours $i-1$, i, and $i+1$, illustrated in Fig. 1.
2. Identify the common perpendicular between the two axes i and $i+1$, or their point of intersection. At the point of intersection, or where the common perpendicular meets the $i+1^{st}$ joint axis, assign the link coordinate system origin, 0_i.
3. For coordinate systems 0 and 1, ensure the coordinate axes are aligned when $\theta_1 = 0$.
4. Assign the z_i axis to point along the joint axis $i+1$.
5. Assign the x_i axis to point along the common normal between the joint axes i and $i+1$. If the axes are parallel, any convenient normal can be selected. If the axes intersect, assign x_i to be perpendicular to the plane containing $z_i - 1$ and z_i.
6. Assign the y_i axis to complete a right-handed coordinate system.

Note that the DH parameters are not unique, i.e., it is possible to attach the coordinate systems in slightly different ways resulting in different sets of DH parameters. For example, when we first align the z_i axis with joint axis $i+1$, there are two choices for this basis vector direction. Regardless of the direction choices made, if one consistently follows these rules the final algebraic IO equation for the RSSR will not differ from the result presented in this paper.

Each of the two S joints of the RSSR can be modelled as three R joints whose rotation axes are mutually orthogonal and intersect at the sphere centre. Hence, eight coordinate frames are attached to the linkage. The chosen coordinate systems are illustrated in Fig. 2 and the corresponding DH parameters are to be found in Tab. 1. Note that the only link twist that is a design parameter is τ_8. The twists between the three mutually orthogonal R joint axes comprising the S joints are $\pm\pi$. We arbitrarily use the positive value, as the sign has no impact on the resulting algebraic IO equation.

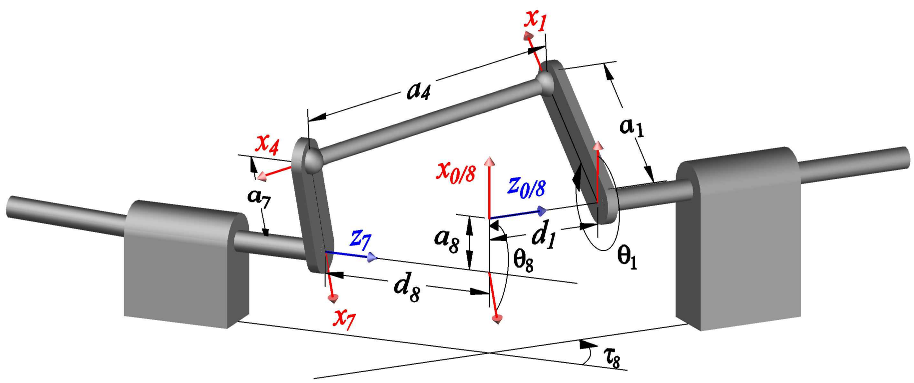

Figure 2: An arbitrary RSSR mechanism.

Table 1: DH parameters for the RSSR mechanism.

joint axis i	joint angle θ_i	link offset d_i	link length a_i	link twist τ_i
1	θ_1	d_1	a_1	0
2	θ_2	0	0	$\pi/2$
3	θ_3	0	0	$\pi/2$
4	θ_4	0	a_4	0
5	θ_5	0	0	$\pi/2$
6	θ_6	0	0	$\pi/2$
7	θ_7	0	a_7	0
8	θ_8	d_8	a_8	τ_8

The DH convention uses two screw displacements to describe the coordinate transformation of joint i relative to joint $i-1$. The two screw displacements consist of one pure rotation, $\mathbf{T}(\theta_i)$ or $\mathbf{T}(\tau_i)$, and one pure translation, $\mathbf{T}(d_i)$ or $\mathbf{T}(a_i)$, each. More precisely, the transformation between two sequential coordinate frames is obtained as

$$ {}_{i}^{i-1}\mathbf{T} = \mathbf{T}(\theta_i) \cdot \mathbf{T}(d_i) \cdot \mathbf{T}(a_i) \cdot \mathbf{T}(\tau_i), \tag{1} $$

where

$$ \mathbf{T}(\theta_i) = \left[\begin{array}{c|ccc} 1 & 0 & 0 & 0 \\ \hline 0 & \cos(\theta_i) & -\sin(\theta_i) & 0 \\ 0 & \sin(\theta_i) & \cos(\theta_i) & 0 \\ 0 & 0 & 0 & 1 \end{array}\right]; \quad \mathbf{T}(d_i) = \left[\begin{array}{c|ccc} 1 & 0 & 0 & 0 \\ \hline 0 & 1 & 0 & 0 \\ 0 & 0 & 1 & 0 \\ d_i & 0 & 0 & 1 \end{array}\right]; $$

$$ \mathbf{T}(a_i) = \left[\begin{array}{c|ccc} 1 & 0 & 0 & 0 \\ \hline a_i & 1 & 0 & 0 \\ 0 & 0 & 1 & 0 \\ 0 & 0 & 0 & 1 \end{array}\right]; \quad \mathbf{T}(\tau_i) = \left[\begin{array}{c|ccc} 1 & 0 & 0 & 0 \\ \hline 0 & 1 & 0 & 0 \\ 0 & 0 & \cos(\tau_i) & -\sin(\tau_i) \\ 0 & 0 & \sin(\tau_i) & \cos(\tau_i) \end{array}\right]. $$

In the remainder of this paper, the tangent half angle substitutions for the angle parameters $v_i = \tan(\theta_i/2)$ and $\alpha_i = \tan(\tau_i/2)$ will be used [22] in order to algebraise the transformations. This implies that

$$ \cos\theta_i = \frac{1-v_i^2}{1+v_i^2}, \quad \sin\theta_i = \frac{2v_i}{1+v_i^2}, \tag{2} $$

$$ \cos\tau_i = \frac{1-\alpha_i^2}{1+\alpha_i^2}, \quad \sin\tau_i = \frac{2\alpha_i}{1+\alpha_i^2}. \tag{3} $$

We begin with a serial RSSR kinematic chain and determine the forward kinematics. The required multiplication of the individual DH transformation matrices from one coordinate frame to another yields the overall homogeneous transformation matrix that describes the relationship between the first and last coordinate frames. To close the kinematic chain, we want the first and last coordinate systems to align in both their orientation and origin. Algebraically, this is specified using the kinematic closure equation, where the overall transformation equates to the identity [16]

$$\prod_{i=1}^{8} {}^{i-1}_{i}\mathbf{T} = \mathbf{I}. \tag{4}$$

The elements of this algebraic DH transformation matrix are then directly mapped into Study's kinematic image space where the constraint manifold could be analysed as it was successfully demonstrated for the planar 4R, spherical 4R, and Bennett linkage [10, 11]. However, applying Gröbner bases or other elimination methods the eight Study soma coordinates to symbolically obtain the IO equation for the RSSR linkage is computationally too demanding for an algebraic geometry approach. While very computationally demanding, a numerical approach that uses the forward kinematics of the serial RSSR chain mapped to the eight soma coordinates, described in Section 5, using pseudowitness sets leads directly to the desired IO equation.

Still, an efficient and elegant algebraic geometry approach, which, for example, has already been successfully applied in [8], is to conceptually split the closure equation in two by multiplying both sides by the inverses of half of the DH transformations. In the case of the RSSR, the closure equation becomes

$$ {}^{0}_{1}\mathbf{T}\,{}^{1}_{2}\mathbf{T}\,{}^{2}_{3}\mathbf{T}\,{}^{3}_{4}\mathbf{T} = \mathbf{I}\,{}^{7}_{8}\mathbf{T}^{-1}\,{}^{6}_{7}\mathbf{T}^{-1}\,{}^{5}_{6}\mathbf{T}^{-1}\,{}^{4}_{5}\mathbf{T}^{-1}. \tag{5}$$

This step essentially divides the linkage into two serial chains joined at the 4th coordinate frame located in the second S joint., i.e., one chain between the coordinate frames 0 and 4, and one chain between the coordinate frames 4 and 8, which correspond to the expressions on the left and right sides of Eq. (5), respectively, which we call the left RS and right RS dyads. Eq. (5) will be used in Section 4 to obtain the algebraic IO equation by projecting it to the image space. However, before we proceed we will briefly recall Study's kinematic mapping [5, 6].

3. Study's Kinematic Mapping

The homogeneous transformation matrices in Eqs. (4) and (5) represent a subgroup of the group of spatial Euclidean displacements, $SE(3)$, with respect to a relatively non-moving coordinate frame. There are several possibilities to parameterise this rigid body displacement group, one of them being the kinematic mapping that was originally formulated by Eduard Study and reported in an appendix of his book "Geometrie der Dynamen" [5] in 1903. It defines every distinct Euclidean displacement as a distinct point on a six-dimensional quadric hyper-surface in a seven-dimensional projective space $\mathbb{P}^7$ now known as the Study quadric, S_6^2. A point on S_6^2 consists of eight homogeneous coordinates, not all zero, $x = [x_0 : x_1 : x_2 : x_3 : y_0 : y_1 : y_2 : y_3]^\intercal$ which Study called a "soma", a Greek word meaning "body". The hyper-surface is a seven-dimensional bilinear hyper-quadratic equation given by

$$x_0y_0 + x_1y_1 + x_2y_2 + x_3y_3 = 0, \tag{6}$$

excluding the *exceptional generator*, which we call A_∞, where $x_0 = x_1 = x_2 = x_3 = 0$, having the parametric representation

$$[0 : 0 : 0 : 0 : y_0 : y_1 : y_2 : y_3].$$

A_∞ does not represent any real displacement, but it nonetheless plays an important role as a generator space. For a soma to represent a real displacement in $SE(3)$, it must satisfy two conditions: the first being Eq. (6); the second being the inequality

$$x_0^2 + x_1^2 + x_2^2 + x_3^2 \quad \neq \quad 0. \tag{7}$$

Eq. (6) contains only bilinear cross terms. This implies that the quadric has been rotated out of its standard position, or normal form [23, 24]. It is straightforward to diagonalise the quadratic form of Eq. (6) which reveals that this six-dimensional quadric in $\mathbb{P}^7$ has the normal form

$$x_0^2 + x_1^2 + x_2^2 + x_3^2 - y_0^2 - y_1^2 - y_2^2 - y_3^2 = 0, \tag{8}$$

which is analogous to the Plücker quadric, P_4^2, of line geometry [25]. The normal form of S_6^2 shows that it is a seven-dimensional hyperboloid of one sheet doubly-ruled by special 3-space generators in two opposite reguli, which we call A-planes and B-planes, after [26].

It can be shown that lines on S_6^2 represent either a one parameter set of translations or rotations [26]. The lines which contain the identity array $[1 : 0 : 0 : \ldots : 0]^T$, which Study called the "protosoma", are either the one parameter rotation or translation subgroups. The exceptional generator A_∞ is an A-plane. In general, two different A-planes do not intersect, nor do two different B-planes, but there are exceptions [27]. An A-plane corresponds to $SO(3)$ if it contains the identity and its intersection with A_∞ is the empty set, and to $SE(2)$ if it contains the identity and intersects A_∞ in a line. These two types of A-planes intersect each other in lines on S_6^2. Each of these lines represent rotations about the line orthogonal to the plane of the planar displacement and through the centre point of the spherical displacement [27, 28]. The only B-planes that intersect A_∞ correspond to the subgroup of all translations. The intersection of an A-plane and a B-plane is either a point, or a two dimensional plane [29].

Given a transformation matrix whose rotation elements are denoted as a_{ij} with $i, j \in \{1, 2, 3\}$ and whose translation vector elements are denoted as t_k with $k \in \{1, 2, 3\}$, then the corresponding Study soma coordinates, also known as Study parameters, are obtained in the following way. The homogeneous quadruple $x_0 : x_1 : x_2 : x_3$ can be obtained from at least one of the following ratios:

$$\begin{aligned} x_0 : x_1 : x_2 : x_3 &= 1 + a_{11} + a_{22} + a_{33} : a_{32} - a_{23} : a_{13} - a_{31} : a_{21} - a_{12}; \\ &= a_{32} - a_{23} : 1 + a_{11} - a_{22} - a_{33} : a_{12} + a_{21} : a_{31} + a_{13}; \\ &= a_{13} - a_{31} : a_{12} + a_{21} : 1 - a_{11} + a_{22} - a_{33} : a_{23} + a_{32}; \\ &= a_{21} - a_{12} : a_{31} + a_{13} : a_{23} + a_{32} : 1 - a_{11} - a_{22} + a_{33}. \end{aligned} \tag{9}$$

The remaining four coordinates $y_0 : y_1 : y_2 : y_3$ are linear combinations of the

x_i and t_i and are computed as

$$\begin{aligned} y_0 &= \tfrac{1}{2}(t_1x_1 + t_2x_2 + t_3x_3), & y_1 &= \tfrac{1}{2}(-t_1x_0 + t_3x_2 - t_2x_3), \\ y_2 &= \tfrac{1}{2}(-t_2x_0 - t_3x_1 + t_1x_3), & y_3 &= \tfrac{1}{2}(-t_3x_0 + t_2x_1 - t_1x_2). \end{aligned} \tag{10}$$

Hence, the mechanical constraints imposed by the type of joints used in the kinematic chains of the RSSR are mapped onto Study's quadric. The result is a parametric represenation in terms of Study soma coordinates of the contraint manifold [30].

The image of the overall DH transformation of the RSSR linkage, Eq. (4), in terms of Study parameters yields

$$\begin{aligned} x_0 &= 2v_1v_2v_3v_4v_5v_6v_7v_8 - 2v_1v_2v_3v_4v_5v_6 + ... + 2\alpha_8v_6v_8 + 2v_7v_8 - 2, \\ x_1 &= 2\alpha_8v_1v_2v_3v_4v_5v_6v_7v_8 - 2\alpha_8v_1v_2v_3v_4v_5v_6 + ... + 2\alpha_8v_7v_8 - 2\alpha_8, \\ x_2 &= -2\alpha_8v_1v_2v_3v_4v_5v_6v_7 - 2\alpha_8v_1v_2v_3v_4v_5v_6v_8 + ... - 2\alpha_8v_7 - 2\alpha_8v_8, \\ x_3 &= -2v_1v_2v_3v_4v_5v_6v_7 - 2v_1v_2v_3v_4v_5v_6v_8 + ... + 2\alpha_8v_6 - 2v_7 - 2v_8, \\ y_0 &= -a_1\alpha_8v_1v_2v_3v_4v_5v_6v_7v_8 + a_4\alpha_8v_1v_2v_3v_4v_5v_6v_7v_8 + ... - \alpha_8a_8, \\ y_1 &= a_1v_1v_2v_3v_4v_5v_6v_7v_8 - a_4v_1v_2v_3v_4v_5v_6v_7v_8 + ... + a_1 + a_4 + a_7 + a_8, \\ y_2 &= -\alpha_8d_1v_1v_2v_3v_4v_5v_6v_7v_8 - \alpha_8d_8v_1v_2v_3v_4v_5v_6v_7v_8 + ... + \alpha_8d_8, \\ y_3 &= -d_1\alpha_8v_1v_2v_3v_4v_5v_6v_7v_8 - d_8v_1v_2v_3v_4v_5v_6v_7v_8 + ... + d_1 + d_8. \end{aligned} \tag{11}$$

As these polynomials are extremely large, each containing 128 very large terms, only the beginning and end of the expressions sorted using graded lexicographic ordering with $v_1 > v_2 > \ldots > v_8$ are displayed here. These polynomials will be solved numerically in Section 5, but are otherwise too cumbersome to deal with using algebraic geometry and computer algebra software, such as Maple 2021. For this we require a different approach.

As mentioned earlier, this different approach involves conceptually splitting the RSSR into two serial RS chains. In this way, mapping the left hand side of Eq. (5), the left RS chain, into Study's kinematic image space yields eight significantly smaller polynomials

$$x_0 = 4v_1v_2v_3v_4 - 4v_1v_3 - 4v_2v_3 - 4v_3v_4,$$

$$
\begin{aligned}
x_1 =& -4v_1v_2 + 4v_1v_4 + 4v_2v_4 + 4,\\
x_2 =& 4v_1v_2v_4 + 4v_1 + 4v_2 - 4v_4,\\
x_3 =& -4v_1v_2v_3 - 4v_1v_3v_4 - 4v_2v_3v_4 + 4v_3, \qquad (12)\\
y_0 =& -2d_1v_1v_2v_3 - 2d_1v_1v_3v_4 - 2d_1v_2v_3v_4 + 2a_1v_1v_2 - 2a_4v_1v_2 - 2a_1v_1v_4\\
&+ 2a_4v_1v_4 + 2a_1v_2v_4 + 2a_4v_2v_4 + 2d_1v_3 + 2a_1 + 2a_4,\\
y_1 =& 2a_1v_1v_2v_3v_4 - 2a_4v_1v_2v_3v_4 + 2d_1v_1v_2v_4 - 2a_1v_1v_3 + 2a_4v_1v_3 + 2a_1v_2v_3\\
&+ 2a_4v_2v_3 + 2a_1v_3v_4 + 2a_4v_3v_4 + 2d_1v_1 + 2d_1v_2 - 2d_1v_4,\\
y_2 =& 2a_1v_1v_2v_3 + 2a_4v_1v_2v_3 + 2a_1v_1v_3v_4 + 2a_4v_1v_3v_4 - 2a_1v_2v_3v_4 + 2a_4v_2v_3v_4\\
&+ 2d_1v_1v_2 - 2d_1v_1v_4 - 2d_1v_2v_4 + 2a_1v_3 - 2a_4v_3 - 2d_1,\\
y_3 =& -2d_1v_1v_2v_3v_4 + 2a_1v_1v_2v_4 + 2a_4v_1v_2v_4 + 2d_1v_1v_3 + 2d_1v_2v_3 + 2d_1v_3v_4\\
&+ 2a_1v_1 + 2a_4v_1 - 2a_1v_2 + 2a_4v_2 + 2a_1v_4 - 2a_4v_4.
\end{aligned}
$$

And finally, mapping the right hand side of Eq. (5), the right RS chain, into Study's kinematic image space yields eight additional smaller polynomials

$$
\begin{aligned}
x_0 =& 4v_5v_6v_7v_8 - 4v_5v_6 - 4\alpha_8v_5v_7 - 4\alpha_8v_5v_8 - 4v_6v_7 - 4v_6v_8 + 4\alpha_8v_7v_8 - 4\alpha_8,\\
x_1 =& -4\alpha_8v_5v_6v_7v_8 + 4\alpha_8v_5v_6 - 4v_5v_7 - 4v_5v_8 + 4\alpha_8v_6v_7 + 4\alpha_8v_6v_8 + 4v_7v_8 - 4,\\
x_2 =& 4\alpha_8v_5v_6v_7 + 4\alpha_8v_5v_6v_8 + 4v_5v_7v_8 + 4\alpha_8v_6v_7v_8 - 4v_5 - 4\alpha_8v_6 + 4v_7 + 4v_8,\\
x_3 =& 4v_5v_6v_7 + 4v_5v_6v_8 - 4\alpha_8v_5v_7v_8 + 4v_6v_7v_8 + 4\alpha_8v_5 - 4v_6 - 4\alpha_8v_7 - 4\alpha_8v_8,\\
y_0 =& -2a_7\alpha_8v_5v_6v_7v_8 + 2a_8\alpha_8v_5v_6v_7v_8 - 2d_8v_5v_6v_7 - 2d_8v_5v_6v_8 - 2\alpha_8d_8v_5v_7v_8\\
&- 2d_8v_6v_7v_8 - 2a_7\alpha_8v_5v_6 - 2a_8\alpha_8v_5v_6 + 2a_7v_5v_7 + 2a_8v_5v_7 - 2a_7v_5v_8\\
&+ 2a_8v_5v_8 - 2a_7\alpha_8v_6v_7 - 2a_8\alpha_8v_6v_7 + 2a_7\alpha_8v_6v_8 - 2a_8\alpha_8v_6v_8 + 2a_7v_7v_8\\
&- 2a_8v_7v_8 + 2\alpha_8d_8v_5 + 2d_8v_6 - 2\alpha_8d_8v_7 - 2\alpha_8d_8v_8 + 2a_7 + 2a_8, \qquad (13)\\
y_1 =& -2a_7v_5v_6v_7v_8 + 2a_8v_5v_6v_7v_8 + 2\alpha_8d_8v_5v_6v_7 + 2\alpha_8d_8v_5v_6v_8 - 2d_8v_5v_7v_8\\
&+ 2\alpha_8d_8v_6v_7v_8 - 2a_7v_5v_6 - 2a_8v_5v_6 - 2a_7\alpha_8v_5v_7 - 2a_8\alpha_8v_5v_7 + 2a_7\alpha_8v_5v_8\\
&- 2a_8\alpha_8v_5v_8 - 2a_7v_6v_7 - 2a_8v_6v_7 + 2a_7v_6v_8 - 2a_8v_6v_8 - 2a_7\alpha_8v_7v_8\\
&+ 2a_8\alpha_8v_7v_8 + 2d_8v_5 - 2\alpha_8d_8v_6 - 2d_8v_7 - 2d_8v_8 - 2a_7\alpha_8 - 2a_8\alpha_8,\\
y_2 =& 2\alpha_8d_8v_5v_6v_7v_8 - 2a_7v_5v_6v_7 - 2a_8v_5v_6v_7 + 2a_7v_5v_6v_8 - 2a_8v_5v_6v_8
\end{aligned}
$$

$$
\begin{aligned}
&- 2a_7\alpha_8 v_5 v_7 v_8 + 2a_8\alpha_8 v_5 v_7 v_8 + 2a_7 v_6 v_7 v_8 - 2a_8 v_6 v_7 v_8 - 2\alpha_8 d_8 v_5 v_6 \\
&- 2d_8 v_5 v_7 - 2d_8 v_5 v_8 - 2\alpha_8 d_8 v_6 v_7 - 2\alpha_8 d_8 v_6 v_8 + 2d_8 v_7 v_8 - 2a_7\alpha_8 v_5 \\
&- 2a_8\alpha_8 v_5 + 2a_7 v_6 + 2a_8 v_6 + 2a_7\alpha_8 v_7 + 2a_8\alpha_8 v_7 - 2a_7\alpha_8 v_8 + 2a_8\alpha_8 v_8 - 2d_8, \\
y_3 = {}& 2d_8 v_5 v_6 v_7 v_8 + 2a_7\alpha_8 v_5 v_6 v_7 + 2a_8\alpha_8 v_5 v_6 v_7 - 2a_7\alpha_8 v_5 v_6 v_8 + 2a_8\alpha_8 v_5 v_6 v_8 \\
&- 2a_7 v_5 v_7 v_8 + 2a_8 v_5 v_7 v_8 - 2a_7\alpha_8 v_6 v_7 v_8 + 2a_8\alpha_8 v_6 v_7 v_8 - 2d_8 v_5 v_6 \\
&+ 2\alpha_8 d_8 v_5 v_7 + 2\alpha_8 d_8 v_5 v_8 - 2d_8 v_6 v_7 - 2d_8 v_6 v_8 - 2\alpha_8 d_8 v_7 v_8 - 2a_7 v_5 - 2a_8 v_5 \\
&- 2a_7\alpha_8 v_6 - 2a_8\alpha_8 v_6 + 2a_7 v_7 + 2a_8 v_7 - 2a_7 v_8 + 2a_8 v_8 + 2\alpha_8 d_8.
\end{aligned}
$$

The polynomials of Eqs. (12) and (13) will be manipulated in Section 4 using the linear implicitisation algorithm [12] to reveal the algebraic RSSR IO equation.

4. Algebraic Geometry Approach

To obtain the RSSR algebraic IO equation, the parametric equations of the Study coordinates of Eqs. (12) and (13) need to be expressed implicitly as a polynomial equation in the desired motion parameters v_1 and v_8 in the seven-dimensional kinematic mapping image space. This requires an algorithm that eliminates the unwanted motion parameters v_i where $i \in \{2, \ldots, 7\}$. One implicitisation algorithm that allows for the transformation from the explicit parametric Study representation into a set of implicit polynomial equations is known as the linear implicitisation algorithm. The resulting constraint equations are implicit polynomials that form an algebraic variety in $\mathbb{P}^7$ and can be manipulated with different tools to obtain the IO equation. A detailed description of the linear implicitisation algorithm, together with illustrative examples is to be found in [6, 12].

The two serial RS chains of the RSSR linkage consist of one revolute and one spherical joint each. Clearly, the S joint spherical displacements, $SO(3)$, are completely contained on sub-spaces of the Study quadric as there is no translation involved and thus, all four y_i Study coordinates are identically zero. In other words, the displacements constrained by the S joints form special A-planes on the Study quadric. Further, the R joint in the serial RS chain rotates the S joint in a planar displacement thereby moving this special A-plane on S_6^2. It is well known that a 3-space can be represented by the intersection of four hyperplanes in the kinematic image space. To determine the RSSR algebraic IO equation we must identify these hyperplanes, one set for each serial RS chain. To obtain their implicit equations the linear implicitisation algorithm will be employed. The main goal of the linear implicitisation algorithm is to find the minimal number of implicit equations that describe the mechanical constraints in the image space. It allows for the elimination of motion parameters which, in the case of the RSSR, correspond to the variables $v_2, v_3, \ldots, v_7$. On the other hand, the design parameters a_i, d_i and α_i are fixed values that depend on the chosen linkage. However, to obtain the implicit polynomials for the spherical special 3-spaces v_1 and v_8 are temporarily also considered as design parameter constants.

To begin, we assume that the resulting variety is defined by linear constraint equations, and hence a general linear *ansatz polynomial* can be written, using the graded reverse lexicographic monomial ordering [31], as

$$C_1y_3 + C_2y_2 + C_3y_1 + C_4y_0 + C_5x_3 + C_6x_2 + C_7x_1 + C_8x_0 = 0. \tag{14}$$

This linear ansatz polynomial has eight unknown coefficients C_i, $i \in \{1, \cdots, 8\}$. In the case of the left hand side of the RSSR chain, Eq. (12) is substituted into Eq. (14) and after reorganising such that the variable angle parameters of the spherical displacement are collected, yields

$$
\begin{aligned}
&(-2C_1d_1v_1 + 2C_3a_1v_1 - 2C_3a_4v_1 + 4C_8v_1 - 2C_4d_1 - 2C_2a_1 + 2C_2a_4 - 4C_5)v_2v_3v_4 \\
&+ (2C_2a_1v_1 + 2C_2a_4v_1 - 2C_4d_1v_1 - 4C_5v_1 + 2C_1d_1 + 2C_3a_1 + 2C_3a_4 - 4C_8)v_2v_3 \\
&+ (2C_1a_1v_1 + 2C_1a_4v_1 + 2C_3d_1v_1 + 4C_6v_1 - 2C_2d_1 + 2C_4a_1 + 2C_4a_4 + 4C_7)v_2v_4 \\
&+ (2C_2d_1v_1 + 2C_4a_1v_1 - 2C_4a_4v_1 - 4C_7v_1 - 2C_1a_1 + 2C_1a_4 + 2C_3d_1 + 4C_6)v_2 \\
&+ (2C_2a_1v_1 + 2C_2a_4v_1 - 2C_4d_1v_1 - 4C_5v_1 + 2C_1d_1 + 2C_3a_1 + 2C_3a_4 - 4C_8)v_3v_4 \\
&+ (2C_1d_1v_1 - 2C_3a_1v_1 + 2C_3a_4v_1 - 4C_8v_1 + 2C_2a_1 - 2C_2a_4 + 2C_4d_1 + 4C_5)v_3 \\
&+ (-2C_2d_1v_1 - 2C_4a_1v_1 + 2C_4a_4v_1 + 4C_7v_1 + 2C_1a_1 - 2C_1a_4 - 2C_3d_1 - 4C_6)v_4 \\
&+ (2C_1a_1v_1 + 2C_1a_4v_1 + 2C_3d_1v_1 + 4C_6v_1 - 2C_2d_1 + 2C_4a_1 + 2C_4a_4 + 4C_7) = 0.
\end{aligned} \tag{15}
$$

To fulfil this equation, the coefficients of the motion parameters in Eq. (15) must vanish since the v_2, v_3, and v_4 orientation angle parameters are, in general non-zero. In matrix form, this can be expressed as

$$
\begin{bmatrix}
2a_1v_1+2a_4v_1 & -2d_1 & 2d_1v_1 & 2a_1+2a_4 & 0 & 4v_1 & 4 & 0 \\
-2d_1v_1 & -2a_1+2a_4 & 2a_1v_1-2a_4v_1 & -2d_1 & -4 & 0 & 0 & 4v_1 \\
-2a_1+2a_4 & 2d_1v_1 & 2d_1 & 2a_1v_1-2a_4v_1 & 0 & 4 & -4v_1 & 0 \\
2a_1v_1+2a_4v_1 & -2d_1 & 2d_1v_1 & 2a_1+2a_4 & 0 & 4v_1 & 4 & 0 \\
2d_1 & 2a_1v_1+2a_4v_1 & 2a_1+2a_4 & -2d_1v_1 & -4v_1 & 0 & 0 & -4 \\
2d_1 & 2a_1v_1+2a_4v_1 & 2a_1+2a_4 & -2d_1v_1 & -4v_1 & 0 & 0 & -4 \\
2d_1v_1 & 2a_1-2a_4 & -2a_1v_1+2a_4v_1 & 2d_1 & 4 & 0 & 0 & -4v_1 \\
2a_1-2a_4 & -2d_1v_1 & -2d_1 & -2a_1v_1+2a_4v_1 & 0 & -4 & 4v_1 & 0
\end{bmatrix}
\begin{bmatrix} C_1 \\ C_2 \\ C_3 \\ C_4 \\ C_5 \\ C_6 \\ C_7 \\ C_8 \end{bmatrix}
=
\begin{bmatrix} 0 \\ 0 \\ 0 \\ 0 \\ 0 \\ 0 \\ 0 \\ 0 \end{bmatrix}.
$$

Solving for the unknown C_i and back-substituting their solutions into the general linear ansatz polynomial Eq. (14) reveals all four hyperplanes that satisfy the variety in $\mathbb{P}^7$. The solution shows that C_1, C_3, C_4, and C_8 are all free parameters with arbitrary values while C_2, C_5, C_6, and C_7 are expressions containing the design parameters and, after simplifying, are each linear in four of the Study parameters, and therefore hyperplanes. These four hyperplanes collected in terms of the Study parameters are

$$
\begin{aligned}
0 &= (a_1^2v_1^2 - a_4^2v_1^2 + d_1^2v_1^2 + a_1^2 - a_4^2 + d_1^2)x_3 + (-2d_1v_1^2 - 2d_1)y_0 \\
&\quad + 4a_1v_1y_1 + (2a_1v_1^2 - 2a_4v_1^2 - 2a_1 - 2a_4)y_2, \qquad (16) \\
0 &= (a_1^2v_1^2 - a_4^2v_1^2 + d_1^2v_1^2 + a_1^2 - a_4^2 + d_1^2)x_2 - 4a_1v_1y_0 + (-2d_1v_1^2 - 2d_1)y_1
\end{aligned}
$$

$$+ (-2a_1v_1^2 + 2a_4v_1^2 + 2a_1 + 2a_4)y_3, \tag{17}$$

$$\begin{aligned} 0 = &(a_1^2v_1^2 - a_4^2v_1^2 + d_1^2v_1^2 + a_1^2 - a_4^2 + d_1^2)x_1 + (2a_1v_1^2 + 2a_4v_1^2 - 2a_1 + 2a_4)y_0 \\ &+ (2d_1v_1^2 + 2d_1)y_2 - 4a_1v_1y_3, \end{aligned} \tag{18}$$

$$\begin{aligned} 0 = &(a_1^2v_1^2 - a_4^2v_1^2 + d_1^2v_1^2 + a_1^2 - a_4^2 + d_1^2)x_0 + (-2a_1v_1^2 - 2a_4v_1^2 + 2a_1 - 2a_4)y_1 \\ &+ 4a_1v_1y_2 + (2d_1v_1^2 + 2d_1)y_3. \end{aligned} \tag{19}$$

The same procedure can be done with the right hand side of the RSSR by substituting Eq. (13) in the general linear ansatz polynomial, Eq. (14). In this case, the motion parameters to be eliminated are v_5, v_6 and v_7. Solving the resulting homogeneous matrix equation for the new unknown C_i yields the following four hyperplanes in a similar way. They are

$$\begin{aligned} 0 = &(a_7^2\alpha_8^2v_8^2 - 2a_7a_8\alpha_8^2v_8^2 + a_8^2\alpha_8^2v_8^2 + \alpha_8^2d_8^2v_8^2 + a_7^2v_8^2 - 2a_8a_7v_8^2 \\ &+ a_8^2v_8^2 + d_8^2v_8^2 + \alpha_8^2a_7^2 + 2a_7a_8\alpha_8^2 + a_8^2\alpha_8^2 + \alpha_8^2d_8^2 + a_7^2 + 2a_7a_8 + a_8^2 + d_8^2)x_3 \\ &+ (-2\alpha_8^2d_8v_8^2 + 2d_8v_8^2 + 8a_7\alpha_8v_8 - 2\alpha_8^2d_8 + 2d_8)y_0 \\ &+ (-4d_8\alpha_8v_8^2 - 4\alpha_8^2a_7v_8 + 4a_7v_8 - 4d_8\alpha_8)y_1 \\ &+ (-2a_7\alpha_8^2v_8^2 + 2\alpha_8^2a_8v_8^2 - 2a_7v_8^2 + 2a_8v_8^2 + 2a_7\alpha_8^2 + 2\alpha_8^2a_8 + 2a_7 + 2a_8)y_2, \end{aligned} \tag{20}$$

$$\begin{aligned} 0 = &(a_7^2\alpha_8^2v_8^2 - 2a_7a_8\alpha_8^2v_8^2 + a_8^2\alpha_8^2v_8^2 + \alpha_8^2d_8^2v_8^2 + a_7^2v_8^2 - 2a_8a_7v_8^2 \\ &+ a_8^2v_8^2 + d_8^2v_8^2 + \alpha_8^2a_7^2 + 2a_7a_8\alpha_8^2 + a_8^2\alpha_8^2 + \alpha_8^2d_8^2 + a_7^2 + 2a_7a_8 + a_8^2 + d_8^2)x_2 \\ &+ (4d_8\alpha_8v_8^2 + 4\alpha_8^2a_7v_8 - 4a_7v_8 + 4d_8\alpha_8)y_0 \\ &+ (-2\alpha_8^2d_8v_8^2 + 2d_8v_8^2 + 8a_7\alpha_8v_8 - 2\alpha_8^2d_8 + 2d_8)y_1 \\ &+ (2a_7\alpha_8^2v_8^2 - 2\alpha_8^2a_8v_8^2 + 2a_7v_8^2 - 2a_8v_8^2 - 2a_7\alpha_8^2 - 2\alpha_8^2a_8 - 2a_7 - 2a_8)y_3, \end{aligned} \tag{21}$$

$$\begin{aligned} 0 = &(a_7^2\alpha_8^2v_8^2 - 2a_7a_8\alpha_8^2v_8^2 + a_8^2\alpha_8^2v_8^2 + \alpha_8^2d_8^2v_8^2 + a_7^2v_8^2 - 2a_8a_7v_8^2 \\ &+ a_8^2v_8^2 + d_8^2v_8^2 + \alpha_8^2a_7^2 + 2a_7a_8\alpha_8^2 + a_8^2\alpha_8^2 + \alpha_8^2d_8^2 + a_7^2 + 2a_7a_8 + a_8^2 + d_8^2)x_1 \\ &+ (-2a_7\alpha_8^2v_8^2 + 2\alpha_8^2a_8v_8^2 - 2a_7v_8^2 + 2a_8v_8^2 + 2a_7\alpha_8^2 + 2\alpha_8^2a_8 + 2a_7 + 2a_8)y_0 \\ &+ (2\alpha_8^2d_8v_8^2 - 2d_8v_8^2 - 8a_7\alpha_8v_8 + 2\alpha_8^2d_8 - 2d_8)y_2 \\ &+ (4d_8\alpha_8v_8^2 + 4\alpha_8^2a_7v_8 - 4a_7v_8 + 4d_8\alpha_8)y_3, \end{aligned} \tag{22}$$

$$
\begin{aligned}
0 = (&a_7^2\alpha_8^2v_8^2 - 2a_7a_8\alpha_8^2v_8^2 + a_8^2\alpha_8^2v_8^2 + \alpha_8^2d_8^2v_8^2 + a_7^2v_8^2 - 2a_8a_7v_8^2 \\
&+ a_8^2v_8^2 + d_8^2v_8^2 + \alpha_8^2a_7^2 + 2a_7a_8\alpha_8^2 + a_8^2\alpha_8^2 + \alpha_8^2d_8^2 + a_7^2 + 2a_7a_8 + a_8^2 + d_8^2)x_0 \\
&+ (2a_7\alpha_8^2v_8^2 - 2\alpha_8^2a_8v_8^2 + 2a_7v_8^2 - 2a_8v_8^2 - 2a_7\alpha_8^2 - 2\alpha_8^2a_8 - 2a_7 - 2a_8)y_1 \\
&+ (-4d_8\alpha_8v_8^2 - 4\alpha_8^2a_7v_8 + 4a_7v_8 - 4d_8\alpha_8)y_2 \\
&+ (2\alpha_8^2d_8v_8^2 - 2d_8v_8^2 - 8a_7\alpha_8v_8 + 2\alpha_8^2d_8 - 2d_8)y_3. \qquad (23)
\end{aligned}
$$

Solving Eqs. (16), ..., (19) for the four y_i and substituting these expressions into Eqs. (20), ..., (23) leaves four equations in the four unknown Study parameters x_i. This suggests solving the system of four equations for the four unknown x_i. However, doing so leads only to the trivial solution $x_i = y_i = 0$, $i \in \{0, 1, 2, 3\}$, which we call the null point. This result can be explained geometrically in $\mathbb{P}^7$ as follows: the two special 3-spaces representing the displacements of the S joints are two $SO(3)$ A-planes that are moved around on S_6^2 under the action of the two R joints, and only ever intersect in the null point.

But, there is a solution. Further inspection of the four equations shows that the equations form a homogeneous system of linear equations. Expressing this linear homogeneous system in matrix-vector form $\mathbf{Ax} = \mathbf{0}$, we know that this system only has a nontrivial solution when the determinant of the 4×4 coefficient matrix $\mathbf{A}$ with respect to the x_i vanishes [32]. Thus, after computing the determinant and omitting the factors that can never vanish, the general algebraic IO equation of the RSSR linkage arises directly from the determinant as

$$
\begin{gathered}
Av_1^2v_8^2 + 8d_1\alpha_8a_7v_1^2v_8 + 8d_8\alpha_8a_1v_1v_8^2 + Bv_1^2 \\
+8a_1a_7(\alpha_8 - 1)(\alpha_8 + 1)v_1v_8 + Cv_8^2 + 8d_8\alpha_8a_1v_1 + 8d_1\alpha_8a_7v_8 + D = 0,
\end{gathered} \qquad (24)
$$

where

$$
\begin{aligned}
A &= (\alpha_8^2 + 1)A_1A_2 + R, \\
B &= (\alpha_8^2 + 1)B_1B_2 + R, \\
C &= (\alpha_8^2 + 1)C_1C_2 + R, \\
D &= (\alpha_8^2 + 1)D_1D_2 + R,
\end{aligned}
$$

and

$$
\begin{aligned}
A_1 &= (a_1 - a_4 + a_7 - a_8), & A_2 &= (a_1 + a_4 + a_7 - a_8),\\
B_1 &= (a_1 + a_4 - a_7 - a_8), & B_2 &= (a_1 - a_4 - a_7 - a_8),\\
C_1 &= (a_1 - a_4 - a_7 + a_8), & C_2 &= (a_1 + a_4 - a_7 + a_8),\\
D_1 &= (a_1 + a_4 + a_7 + a_8), & D_2 &= (a_1 - a_4 + a_7 + a_8),
\end{aligned}
$$

$$R = (d_1 - d_8)^2\alpha_8^2 + (d_1 + d_8)^2.$$

Eq. (24) is an implicit biquadratic algebraic curve of degree 4 in the joint angle parameters v_1 and v_8, as one would expect.

5. Numerical Approach

The degree four algebraic IO equation for the RSSR expressed as Eq. (24) will be compared to the result from a concomitant numerical method. The aim for the numerical method is to compute an eliminant with the general approach of numerical elimination theory [33, Ch. 16]. This involves performing computations using the given polynomial system from Eq. (11) and geometrically projecting points via pseudowitness sets [34]. For this problem, the pseudowitness set provided that the degree of the eliminant is 8 in 9 variables $(v_1, v_8, \alpha_8, a_1, a_4, a_7, a_8, d_1, d_8)$. Since there are a total of $\binom{9+8}{8} = 24310$ monomials of degree at most 8 in 9 variables, the approach is to use the pseudowitness set to generate at least 24310 sample points and then to use interpolation to recover the eliminant [35, Ch. 6]. To gather these sample points, one randomly fixes values of the parameters $\alpha_8, a_1, a_4, a_7, a_8, d_1, d_8$, and solves for the angle parameter values, v_1 and v_8 using any of a variety of sampling methods within numerical algebraic geometry [36, Sec. 2.3]. This yields precisely the same IO equation as the LIA approach, Eq. (24).

6. Geometric Verification

To verify both the algebraic and numerical results, the IO equation of an arbitrary linkage was animated in GeoGebra. The model enabled measurement of the output angle for any given input angle. Tracing the locus of each input-output pair results in a curve which is compared with the herein derived IO equation, Eq. (24). The chosen design parameters for the example linkage are $a_1 = 3$, $a_4 = 5$, $a_7 = 9$, $d_8 = 3$, $a_8 = 11$ and $\tau_8 = 60°$. While the result of the

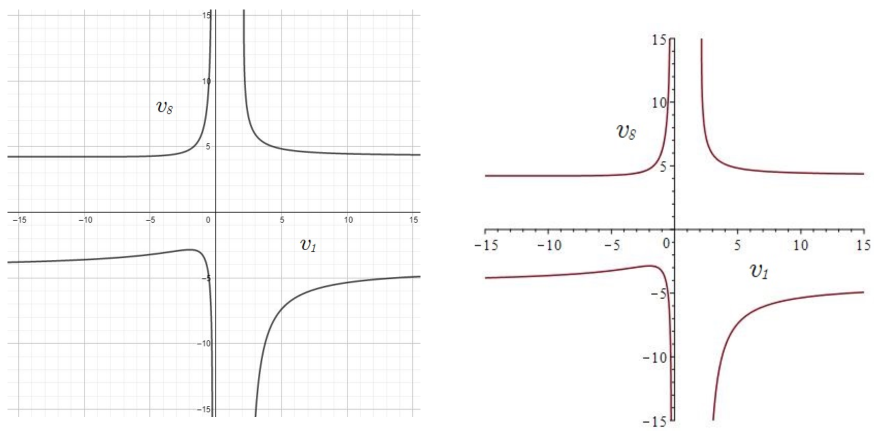

(a) IO equation geometrically generated in GeoGebra.

(b) Derived IO equation according to Eq. (24).

Figure 3: Example RSSR function generator with $a_1 = 3$, $a_4 = 5$, $a_7 = 9$, $d_8 = 3$, $a_8 = 11$ and $\tau_8 = 60°$.

GeoGebra file is displayed in Fig. (3a), substituting the same design parameters into Eq. (24) yields the curve in Fig. (3b). As can be seen, the curves are congruent which further suggests that Eq. (24) is indeed correct.

7. Relation to the IO equation of the Planar 4R Linkage

Following [4, Sec. 11.4] the IO equation of the RSSR linkage can be directly transformed into the IO equation of the planar 4R linkage since the planar 4R is a special case of the RSSR. This requires substituting $\alpha_8 = d_1 = d_8 = 0$ into Eq. (24). After renaming the link lengths and the output angle such that the coupler becomes a_2, the output link a_3, the base link a_4, and the angle of the output v_4 instead of the notation from Fig. (2), i.e., a_4, a_7, a_8, and v_8, respectively, the RSSR IO equation reduces to

$$Av_1^2v_4^2 + Bv_1^2 - 8a_1a_3v_1v_4 + Cv_4^2 + D = 0, \tag{25}$$

where

$$\begin{aligned} A &= (a_1 - a_2 + a_3 - a_4)(a_1 + a_2 + a_3 - a_4) = A_1 A_2, \\ B &= (a_1 + a_2 - a_3 - a_4)(a_1 - a_2 - a_3 - a_4) = B_1 B_2, \\ C &= (a_1 - a_2 - a_3 + a_4)(a_1 + a_2 - a_3 + a_4) = C_1 C_2, \\ D &= (a_1 + a_2 + a_3 + a_4)(a_1 - a_2 + a_3 + a_4) = D_1 D_2, \end{aligned}$$

which is the same IO equation as derived in [10] for planar 4R linkages.

8. Conclusions

In recent publications [10, 11] it was shown that Study's kinematic image space and elimination theory provide an excellent, straight forward tool to derive algebraic IO equations for planar, spherical, and Bennett linkages. In this paper, the same method was extended to arbitrary spatial four-bar linkages, namely the RSSR. After describing the linkage with standard DH parameters and mapping the closure equation into Study's kinematic image space, the intermediate motion parameters were eliminated with two concomitant methods: algebraically using the linear implicitisation algorithm; and numerically using pseudowitness sets to generate points and then interpolation to recover the eliminant. Both methods lead to the same IO equation containing four more complicated coefficients of the input and output angles compared to the planar 4R, but clearly containing the algebraic IO equation of planar 4R linkages as a subset. This IO equation was additionally verified using a geometric animation in GeoGebra. It is intriguing to consider further investigation of the structure of the herein derived algebraic IO equation, how it relates to the linkage mobility, coupler motion, and how it can be used for type and dimensional continuous algebraic synthesis.

Acknowledgements

The authors thank Jonathan Hauenstein for helpful discussions regarding numerical computation methods. Martin Pfurner is also acknowledged for thoughtful contributions to our understanding of S_6^2. The authors also acknowledge the financial support of the Natural Sciences and Engineering Research Council of Canada (NSERC).

References

[1] L. Birglen, T. Laliberté, C. Gosselin, Underactuated Robotic Hands, Springer-Verlag, Berlin, Germany, 2008.

[2] C. M. Gosselin, J.-F. Hamel, The Agile Eye: a High-performance Three-degree-of-freedom Camera-orienting Device, in: Proceedings of the 1994 IEEE International Conference on Robotics and Automation, Vol. 1, 1994, pp. 781–786. doi:10.1109/ROBOT.1994.351393.

[3] F. Freudenstein, Design of Four-link Mechanisms, Ph.D. thesis, Columbia University, New York, NY, U.S.A. (1954).

[4] J. M. McCarthy, G. S. Soh, Geometric Design of Linkages, 2nd Edition, Interdisciplinary Applied Mathematics, Springer, New York, NY, U.S.A., 2011. doi:10.1007/978-1-4419-7892-9.

[5] E. Study, Geometrie der Dynamen, Teubner Verlag, Leipzig, Germany, 1903.

[6] M. L. Husty, D. R. Walter, Mechanism Constraints and Singularities - the Algebraic Formulation, CISM International Centre for Mechanical Sciences 589, Springer International Publishing, Cham, Switzerland, 2019, pp. 101–180. doi:10.1007/978-3-030-05219-5_4.

[7] M. L. Husty, An Algorithm for Solving the Direct Kinematics of General Stewart-Gough Platforms, Mechanism and Machine Theory 31 (4) (1996) 365–379. doi:10.1016/0094-114X(95)00091-C.

[8] M. Pfurner, T. Stigger, M. L. Husty, Algebraic Analysis of Overconstrained Single Loop Four link Mechanisms with Revolute and Prismatic Joints, Mechanism and Machine Theory 114 (2017) 11–19. doi:10.1016/j.mechmachtheory.2017.03.014.

[9] A. J. Sommese, C. W. Wampler, The Numerical Solution Of Systems Of Polynomials Arising In Engineering And Science, World Scientific Publishing Co. Pte. Ldt., Hackensack, NJ, U.S.A., 2005.

[10] M. Rotzoll, M. J. D. Hayes, M. L. Husty, M. Pfurner, A General Method for Determining Algebraic Input-Output Equations for Planar and Spherical 4R Linkages, in: J. Lenarčič, B. Siciliano (Eds.), Advances in Robotic Kinematics 2020, Springer International Publishing, Cham, Switzerland, 2021, pp. 90–97. doi:10.1007/978-3-030-50975-0_12.

[11] M. Rotzoll, M. J. D. Hayes, A General Method for Determining Algebraic Input-output Equations for the Slider-crank and the Bennett Linkage, 11th CCToMM Symposium on Mechanisms, Machines, and Mechatronics, Ontario Tech University, Oshawa, ON, Canada, 2021.

[12] D. R. Walter, M. L. Husty, On Implicitization of Kinematic Constraint Equations, Machine Design & Research (CCMMS 2010) 26 (2010) 218–226.

[13] J. J. Uicker, G. R. Pennock, J. E. Shigley, Theory of Machines and Mechanisms, 5th Edition, McGraw-Hill, New York, NY, U.S.A., 2016.

[14] R. S. Hartenberg, J. Denavit, Kinematic Synthesis of Linkages, McGraw-Hill, New York, NY, U.S.A, 1964.

[15] K. H. Hunt, Kinematic Geometry of Mechanisms, Clarendon Press, Oxford, England, 1978.

[16] J. Denavit, R. S. Hartenberg, A Kinematic Notation for Lower-Pair Mechanisms Based on Matrices, ASME J. Appl. Mech. 22 (2) (1955) 215–221. doi:10.1115/1.4011045.

[17] J. Craig, Introduction to Robotics, Mechanics and Control, 4th Edition, Addison-Wesley Publishing Co., Reading, MA, U.S.A., 2017.

[18] B. Mooring, Z. Roth, M. Driels, Fundamentals of Manipulator Calibration, John Wiley & Sons, Inc., New York, NY, U.S.A., 1991.

[19] C. H. An, C. G. Atkeson, J. M. Hollerbach, Model-based Control of a Robot Manipulator, The MIT Press, Cambridge, MA, U.S.A., 1988.

[20] S. Hayati, Robot Arm Geometric Link Parameter Estimation, Proc. 22nd IEEE Conf. on Decision and Control, San Antonio, TX, U.S.A. (1983) 1477–1483.

[21] M. Husty, M. Pfurner, H.-P. Schröcker, A New and Efficient Algorithm for the Inverse Kinematics of a General Serial 6R Manipulator, Mechanism and Machine Theory 47 (2007) 66–81.

[22] G. L. Bradley, K. J. Smith, Calculus, Prentice Hall, Englewood Cliffs, NJ, U.S.A., 1995.

[23] B. Odehnal, H. Stachel, G. Glaeser, The Universe of Quadrics, Springer-Verlag GmbH, Berlin, Germany, 2020.

[24] H. Anton, Elementary Linear Algebra, John Wiley and Sons, Inc., New York, NY, U.S.A, 1987.

[25] H. Pottmann, J. Wallner, Computational Line Geometry, Springer Verlag, Berlin, Germany, 2001.

[26] J. M. Selig, Geometric Fundamentals of Robotics, 2nd Edition, Springer Science + Business Media Inc, New York, NY, U.S.A., 2005.

[27] J. M. Selig, On the Geometry of the Homogeneous Representation for the Group of Proper Rigid-body Displacements, Rom. J. Techn. Sci. – Appl. Mechanics 58 (1-2) (2013) 153–176.

[28] M. Pfurner, The Family of Two Generator 3-Space Rulings of the Study Quadric, Private Communication (August 25, 2022).

[29] M. L. Husty, H.-P. Schröcker, Kinematics and Algebraic Geometry, in: J. M. McCarthy (Ed.), 21st Century Kinematics, Springer-Verlag, London, 2013, pp. 85–123. doi:10.1007/978-1-4471-4510-3_4.

[30] M. L. Husty, M. Pfurner, H.-P. Schröcker, K. Brunnthaler, Algebraic Methods in Mechanism Analysis and Synthesis, Robotica 25 (6) (2007) 661–675. doi:10.1017/S0263574707003530.

[31] D. A. Cox, J. Little, D. O'Shea, Using Algebraic Geometry, 2nd Edition, Springer Science + Business Media Inc., New York, NY, U.S.A., 2004.

[32] A. Dresden, Solid Analytic Geometry and Determinants, John Wiley & Sons, Inc., New York, NY, U.S.A., 1930.

[33] D. J. Bates, A. J. Sommese, J. D. Hauenstein, C. W. Wampler, Numerically Solving Polynomial Systems with Bertini, SIAM, Philadelphia, PA, U.S.A., 2013. doi:10.1137/1.9781611972702.

[34] J. D. Hauenstein, A. J. Sommese, Witness Sets of Projections, Applied Mathematics and Computation 217 (7) (2010) 3349–3354. doi:10.1016/j.amc.2010.08.067.

[35] D. Kincaid, W. Cheney, Numerical Analysis: Mathematics of Scientific Computing, American Mathematical Society, Provedince, RI, U.S.A., 2002.

[36] D. A. Cox, Applications of Polynomial Systems, Vol. 134, CBMS Regional Conference Series in Mathematics, American Mathematical Society, Providence, RI, U.S.A., 2020.